Marine Geology 441 (2021) 106635

Contents lists available at ScienceDirect

Marine Geology

journal homepage: www.elsevier.com/locate/margo

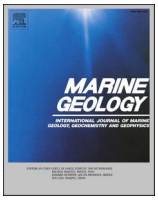

The geologic record of Hurricane Irma in a Southwest Florida back-barrier lagoon

Tynisha Martin [*,1], Joanne Muller

Department of Marine and Earth Sciences, Florida Gulf Coast University, Fort Myers, FL, USA

ARTICLE INFO

Keywords:
Paleotempestology
Overwash
Storm-surge
Barrier Island
Gulf of Mexico
Hurricane Irma

ABSTRACT

On 10 September 2017, Category 3 Hurricane Irma made landfall along the Southwest Florida coastline between Cape Sable and Cape Romano. Geologic evidence of this storm is preserved in a back-barrier lagoon behind the Big Hickory Barrier Island, which is located ~64 km north of the landfall point and is positioned 43–65 m east of the Gulf of Mexico. Modern dune height is ~0.83–0.88 m, which was exceeded by the storm surge (recorded height 0.9–1.5 m) allowing for sediment deposition in the Big Hickory Island Lagoon. Geologic evidence is likely found at this location due to proximity to the Gulf of Mexico and the shallow barrier itself. Three cores were analyzed for moisture, inorganic content, grain size, and foraminiferal assemblages. The presence of a hurricane signature (tempestite) is evident in the uppermost horizon of all the cores and includes a fining upward trend of medium sand to clay against a background of organics and fine-grained sediments. Tempestite layers were thicker behind narrower sections of the beach, indicating preferential back-barrier deposition behind narrow barrier sections. Several different foraminiferal species within the tempestite sediments corroborate a marine sediment origin. In addition, historic satellite imagery shows that the Big Hickory Barrier Island is very susceptible to geomorphological change through time, especially due to storm impacts. This research demonstrates the utility of back-barrier sediment cores in understanding hurricane history and barrier island vulnerability.

1. Introduction

In the United States hurricanes are the most costly and deadly natural disaster (Diaz and Pulwarty, 1997; Emanuel, 2005; Smith and Matthews, 2015). Expected annual economic losses caused by hurricane winds and storm-related flooding are estimated at $54 billion (Congressional Budget Office, 2019). Hurricanes are also responsible for the highest number of deaths: 6593 between 1980 and 2020 (Nordhaus, 2010; Jung et al., 2014; Smith and Matthews, 2015; Congressional Budget Office, 2019). Due to the impacts of climate change, which include accelerated sea-level rise, increased sea surface temperatures and increased atmospheric water vapor, hurricane damages are expected to increase in the future. The 2017 hurricane season was the costliest to date with 17 named storms, 10 hurricanes and 6 major hurricanes (Klotzbach et al., 2018). Damages are estimated at $306.2 billion, largely due to three storms – Hurricanes Harvey, Irma, and Maria (Halverson, 2018).

Coastal population and exposure growth is also a driver of increased hurricane damage costs. Between July 2010 and July 2019, the population growth rate of Florida was 14.2% (United States Census Bureau, 2019). Fort Myers, one of the fastest growing Floridian cities, increased in population by approximately 40% between 2010 and 2019 (United States Census Bureau, 2019). This low-lying region is situated on a coastline dominated by barrier islands, of which many are "critically eroded" (e.g., Lee County has 11 critically eroded beaches). Inundation by hurricane storm surge is the leading natural threat to this coastal community. In this region the potential for hurricane inundation is expected to be amplified in the future, as the barrier islands themselves are vulnerable to degradation from climate induced sea-level rise. This potential escalation in hurricane flood inundation can lead to an increased land area threatened by storm surge, potentially increasing hurricane-induced economic damages (Irish et al., 2010).

In 2017 Hurricane Irma made landfall in Southwest Florida as a strong Category 3 storm. The storm had weakened to a Category 2 as it reached the Fort Myers area. The combined effect of the storm surge and tide produced maximum inundation levels of 0.9–1.5 m above ground level (Cangialosi et al., 2018). Even though this storm was a category 2 at landfall it still had significant erosive power with erosive conditions ranging from 1 to 5 in Lee and Collier Counties (Florida Department of Environmental Protection, 2018). Hurricane Irma was the fifth-costliest

* Corresponding author.
E-mail address: trmartin1@usf.edu (T. Martin).
[1] Now at College of Marine Science, University of South Florida, Saint Petersburg, FL, USA.

https://doi.org/10.1016/j.margeo.2021.106635
Received 15 July 2021; Received in revised form 7 September 2021; Accepted 10 September 2021
Available online 15 September 2021

hurricane of all time (Cangialosi et al., 2018) at ~$50 billion in damages.

It is crucial to understand how future hurricanes will impact this highly populated, hurricane-prone region. This study incorporates a field of study termed "paleotempestology" to look at Hurricane Irma's overwash at back-barrier field sites in Estero Bay, Florida (Fig. 1). Historic aerial imagery is also utilized to look at barrier island changes through time. The main goal of this research is to look at the effects of storm surge overwash and erosion along the Southwest Florida coast to gain a better understanding of the potential future impacts of hurricanes on this highly populous coastline.

1.1. Paleotempestology

High-intensity storms (i.e., hurricanes) often carry large, suspended sediment loads that can be deposited in various locations (Plant and Stockdon, 2012; Landsea et al., 2014). When a storm originates in deeper water, it has the potential to deposit deep-sea sediment on the beach face or farther inland. The most severe storms will cause dune erosion and overwash fans through landward sediment transport (Plant and Stockdon, 2012). Most paleotempestological records are created using preserved hurricane overwash signatures (Liu and Fearn, 1993; Risi et al., 1995; Liu and Fearn, 2000). In these studies, the combination of storm surge and waves over-topping barrier islands produces overwash signatures in back-barrier environments (Schwartz, 1975; Donnelly et al., 2001; Buynevich et al., 2004; Woodruff et al., 2008). Some of the best sites for preserving overwash deposits as archives of hurricane landfalls are coastal lakes, lagoons, and marshes (Liu and Fearn, 1993; Hippensteel and Martin, 1999; Liu and Fearn, 2000; Donnelly et al., 2001, 2004; Buynevich and Donnelly, 2006; Lin et al., 2014). The sediment and microfossils from these locations have been used to document prehistoric storm frequency and recurrence intervals (Hippensteel and Martin, 1999; Donnelly et al.,

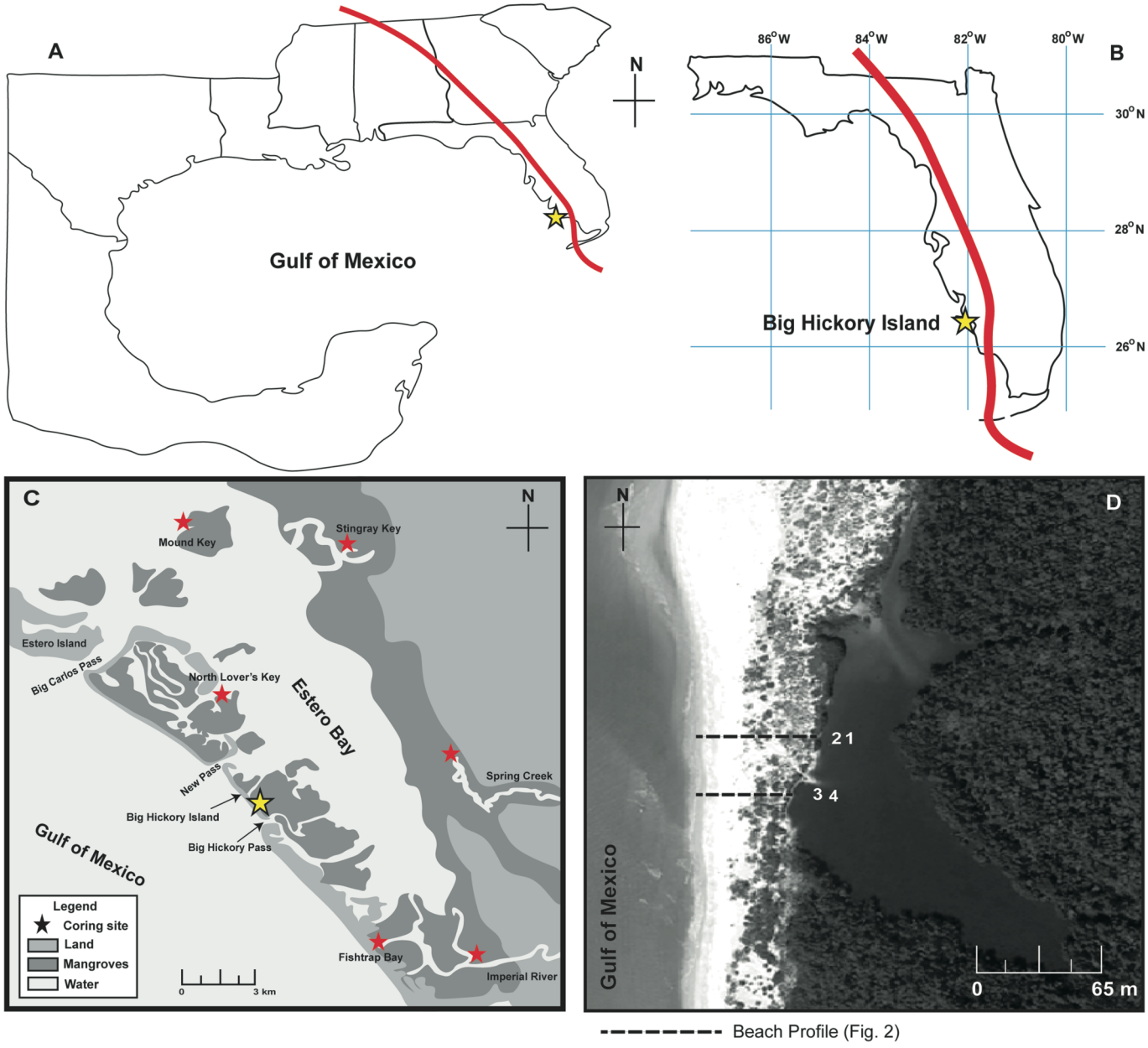

Fig. 1. A) Map of the Gulf of Mexico and surrounding states, including the path of Hurricane Irma in red. B) Map of the state of Florida, highlighting Big Hickory Island. C) Map of Estero Bay, including coring sites. The yellow star indicates the Big Hickory Island Lagoon. D) Site map of the lagoon, highlighting cores BH1, BH2, BH3, and BH4. (For interpretation of the references to colour in this figure legend, the reader is referred to the web version of this article.)

2001; Scott et al., 2003; McCloskey and Keller, 2009; Lane et al., 2011). Studies are lacking in the Southwest Florida region, with only one published record (Ercolani et al., 2015).

2. Study area

Estero Bay is located 32 km south of Fort Myers, FL (Fig. 1). This ~48 km^2 brackish bay receives semidiurnal tidal influx through four tidal inlets between barrier islands: Big Carlos, Matanzas, New Pass, and Big Hickory (Byrne and Gabaldon, 2008). Fresh water enters through three drainage basins: Hendry/Mullock Creeks, the Estero River, and the Imperial River (Wohlpart et al., 2007). The bordering barrier islands protect the bay from open-ocean processes and major storm events (Wohlpart et al., 2007). Previous studies have shown that since the barrier islands formed ~4800 years ago, Estero Bay has become an increasingly protected environment (Wohlpart et al., 2007). Sediment cores taken in the middle of the bay show a fining-upward sequence as well as poorer sorting closer to the surface, indicating a change from an open, high-energy marine environment to a lower energy, estuarine environment (Wohlpart et al., 2007). Older sediments are supratidal and subaerial in nature, meaning that the environment was dry land at that time. Younger sediments are more consistent with mangrove and bay deposits (Obley et al., 2001).

The barrier islands of Estero Bay were formed by longshore currents and exhibit a north-south orientation. They are largely composed of quartz sand on the Gulf side and mangrove forests on the bay side (Wohlpart et al., 2007). The islands were formed due to a wave-dominated Southwest Florida coast, an abundant sediment supply, and a relatively low shelf gradient offshore (Smith et al., 2010). The inlets between islands are considered ephemeral, often closing in as short a period as 1 year (Byrne and Gabaldon, 2008); however, recently they have been kept open by dredging, which allows boat traffic to pass between islands. During storm events, high energy currents can disperse coarse-grained sediment from the Gulf of Mexico throughout the entirety of Estero Bay (average depth: 0.91 m) either via sediment transport through inlets or overwashing of the barrier islands (Byrne and Gabaldon, 2008). The primary coring location of this study was a small back-barrier lagoon (26°22′15.92″ N, 81°51′49.28″ W) located behind the dune and foreshore of the Big Hickory Barrier Island complex, which is one of multiple barrier islands that separate Estero Bay from the Gulf of Mexico (Fig. 1C). Presently the barrier island sees dominant northerly waves, and therefore a dominant northerly longshore drift pattern. The average diurnal range is 0.76 m (Carlos Point Station ID: 8725325). The Big Hickory Barrier Island is located ~64 km north of Hurricane Irma's point of initial landfall and is located 43–65 m from the Gulf of Mexico, shielded by a shallow dune (Fig. 1D). Presently, the lagoon is cut off from both the Gulf of Mexico and Estero Bay, facilitating organic-rich, soft sand seafloors. However, in recent history the lagoon has been open to both Estero Bay and the Gulf of Mexico and therefore has been under tidal and marine influence in the past. Sediment cores were taken throughout Estero Bay for comparison (Fig. 1C).

3. Methods

3.1. Profiling and sampling

On 21 June 2018 a theodolite, tripod and staff were used to obtain two beach profiles seaward of the Big Hickory Island Lagoon to determine the relative vulnerability of the site to storm overwash (Figs. 1D and 2). A base elevation on these transects was established using a Trimble RTK unit, model 8A and calibrated it to NAVD88 datum. Unfortunately, beach profile data are not available for pre-Hurricane Irma. To compensate, LiDAR data from 2015 were used to compare beach face changes. LiDAR data were extracted from NOAA Digital Coast archives, courtesy of USGS (https://coast.noaa.gov/dataviewer/#/lidar/search/).

Seven coring sites were chosen after the landfall of Hurricane Irma for preliminary coring (Fig. 1C). Fishtrap Bay, North Lovers Key Lagoon, Mound Key Entrance, Imperial River Offshoot, Spring Creek, Stingray Key and Big Hickory Island Lagoon were cored in search of a Hurricane Irma signature. Big Hickory Island Lagoon was chosen to be the focus site for this study and, therefore, four cores within the Big Hickory Island Lagoon were taken. All cores were geolocated using a Trimble RTK differential GPS unit (Fig. 1D). Cores BH1 and BH2 are in a transect from the bank of the lagoon toward the center of the lagoon, whereas cores BH3 and BH4 were taken in alignment with the overwash fan created by Hurricane Irma in 2017. Cores were taken by hand-coring technique (Ginsburg and Lloyd, 1956), using a 7.5 cm diameter aluminum pipe and detachable handles. To account for sediment compaction, the height of the sediment outside the pipe was subtracted from that on the inside (Ercolani et al., 2015).

3.2. Sedimentary analyses

Cores were photographed and sediment composition and grain size were determined using known standards. Stratigraphic profiles were subsequently constructed. All cores taken at this site showed no signs of bioturbation or sediment deformation. Percent inorganic content, percent moisture, and grain size analyses were performed on samples taken every 1 cm throughout the uppermost sediments. Samples ~2 cm^3 in size were extracted from each core, dried, and weighed and placed in the muffle furnace at 500°C for 4 h to burn off organic material before being weighed again. This weight was used to calculate the percent loss

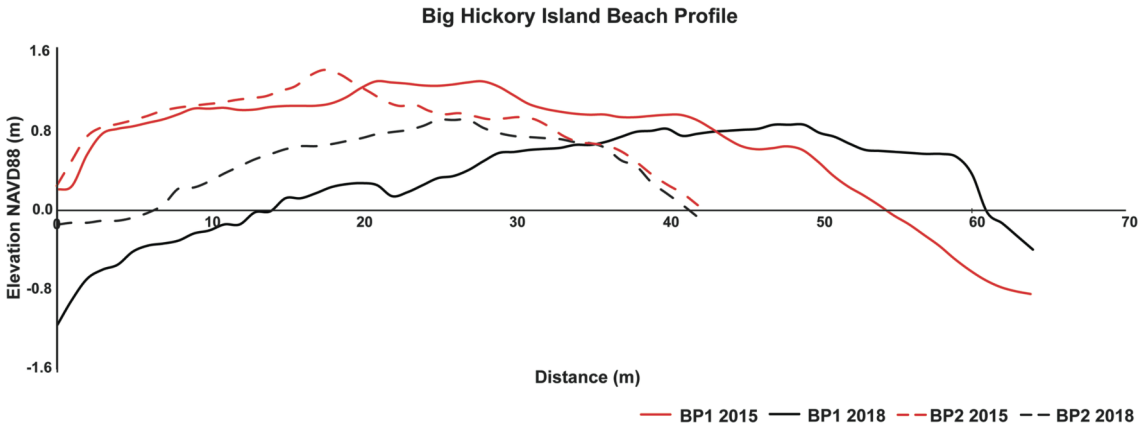

Fig. 2. Beach profiles of the Big Hickory Barrier Island. The black line indicates BP1, which was in transect with cores BH1 and BH2. The black, dashed line indicates BP2, which was in transect with cores BH3 and BH4. The red and red, dashed lines indicate LIDAR data from 2015. MSL is 0.138 m below NAVD88 at this site. (For interpretation of the references to colour in this figure legend, the reader is referred to the web version of this article.)

on ignition (LOI). LOI was determined using the fraction of the furnace weight divided by the dry weight of the sample, expressed as a percentage. Samples were then dry sieved using a 125-μm sieve to determine percentage by volume of sediment coarser than 125 μm.

To assess foraminifera species assemblages a sub-sample was taken from both the tempestite and lagoonal sediments in cores BH1, BH2, and BH3 (at intervals 1–2 cm, 11–12 cm, and 18–19 cm). Samples were sieved through 63-μm and 112-μm mesh sieves using deionized water and left to dry in the oven overnight. The dried sample was disaggregated if necessary and thoroughly mixed. Each sample was then run through a sample splitter 32 times. The weighed subsample was evenly distributed over a gridded picking tray and examined using a stereomicroscope. All foraminifers in readily identifiable condition (i.e., heavily worn and reworked specimens were excluded) were picked onto a cardboard micropaleontological slide, and a preliminary count was made. If the number of specimens picked was ~150–200, the subsample was sufficient. If fewer specimens were picked in the first portion, then a second subsample was taken and picked. The samples were sorted for species, counted, and recorded in a spreadsheet. The percentage of specimens for each species group was calculated by summing the specimens of each species of that sub-sample and dividing by the total number of specimens counted. Therefore, species number fraction is displayed as a percentage.

3.3. Radiometric dating

The sediment core chronology relies on ^{210}Pb radiometric dating. Bulk samples were taken at 0.5 cm intervals in the uppermost 2 cm of core, then at 0.5 cm sample intervals every 1 cm between 2 and 14 cm. The sample preparation, radioactive counting, and modeling for ^{210}Pb-based sediment dating have been previously described by Adhikari et al. (2016). Briefly, the sediment samples were weighed to determine the wet weight, dried at 60°C in an oven, and then weighed again to determine the dry weight, from the difference in the moisture content of the samples. Following this, the aliquots were weighed and ground with a mortar and pestle. Approximately 28 to 32 g of dried/ground sediments were placed into counting vials of known geometry and sealed before measuring for ^{210}Pb and ^{226}Ra (via ^{214}Pb) through direct counting using a SAGe High-Purity Germanium Well Detector (Adhikari et al., 2016). All activities were corrected for decay to the midpoint of sample collection. Unsupported ^{210}Pb ($^{210}Pb_{ex}$) was calculated as the difference between the measured total ^{210}Pb at 46.5 keV and the estimate of the supported ^{210}Pb activity given by its parent nuclide ^{214}Pb at 351 keV [$^{210}Pb_{ex} = {}^{210}Pb_{tot} - {}^{214}Pb$].

The sedimentation and sediment accumulation rates were calculated using the Constant Rate of Supply (CRS) model (Binford, 1990). The CRS model allows sedimentation rates to vary over time and is thus more applicable for shallow Southwest Florida coastal-marine environments where large anthropogenic activities alter the sediment loads (Appleby and Oldfield, 1992; Lubis, 2013; Adhikari et al., 2016). Three assumptions were made using this model: 1) Constant fallout of ^{210}Pb (unsupported ^{210}Pb) from the atmospheric to the sediments, irrespective of any variations which may have occurred in the sediment accumulation rates thus, permits a variable sediment supply (Appleby and Oldfield, 1978; Krishnaswamy et al., 1971; Lubis, 2013); 2) Change in the accumulation rate of bulk sediment dilutes or concentrates the sedimentary ^{210}Pb (Appleby and Oldfield, 1983; Binford and Brenner, 1986); 3) There is instantaneous and complete mixing within the sediment zone. There is no mixing among different sediment zones. Errors were calculated using first-order analysis following Binford (1990).

4. Results

4.1. Beach profiling

Beach Profile 1 (BP1) was taken in transect with cores BH1 and BH2, and shows a beach width of 65 m and a maximum barrier height of 0.83 m. Beach Profile 2 (BP2) was taken in transect with cores BH3 and BH4, and shows a beach width of 43 m and a maximum barrier height of 0.88 m. To assess recent changes to barrier island morphology, beach profile data were extracted from the available 2015 LIDAR data for Big Hickory Barrier Island (shown in red in Fig. 2) and compared to the 2018 data. Between 2015 and 2018 there have been major changes to the dune and foreshore morphology. These was a substantial reduction in the overall maximum height of the beach profile from 5 m in 2015 to 0.88 m in 2018. Beach profiles also indicate a landward migration of the foreshore and dune.

4.2. Stratigraphy and sedimentology of sediment cores

To document the overwash of Hurricane Irma a series of cores were taken post Hurricane Irma landfall. Cores were taken in Fishtrap Bay, North Lovers Key Lagoon, Mound Key Entrance, Imperial River Offshoot, Spring Creek, Stingray Key and Big Hickory Island Lagoon (Fig. 1C). Core photographs were taken, and stratigraphic logs were composed for these sites (Figs. 3 and 4). Cores from Fishtrap Bay, Mound Key Entrance, and Stingray Key were composed of organic-rich, fine-grained silts indicative of lagoonal sediments. The core from Stingray Key has a sandy shell hash layer from 10 to 18 cm before returning to an organic-rich, fine-grained silt. Cores from North Lovers Key Lagoon and Imperial River Outshoot have peat in the core top (to 20 cm and 10 cm, respectively) followed by a sandy, shell hash layer below. The top of the Spring Creek core was composed of silt to 12 cm, followed by a medium to coarse-grained sandy layer. None of the sites in this study showed signs of a Hurricane Irma tempestite, except for the Big Hickory Island Lagoon site. As a result, the Big Hickory Island Lagoon was chosen as the focus of this study.

Big Hickory Island Lagoon cores BH1, BH2 and BH3 were used for sedimentology analyses and BH4 for ^{210}Pb dating. No noticeable signs of bioturbation or sediment deformation from coring were observed. Distinct facies changes were noted. A coarse-grained layer was clearly observed in the upper sediments (Figs. 5 and 6) however varies in thickness (BH1 = 4.0 cm, BH2 = 3.0 cm, BH3 = 9.5 cm, BH4 = 2.0 cm) (Fig. 5). The coarse layer was primarily composed of fine-medium sand quartz, small amounts of calcareous shell hash (<5%) and clay. The clays give the layer a gray coloring (Fig. 6), where core BH2 was dark gray and slightly darker in colour than cores BH1 and BH3, which were light gray and grayish olive, respectively. Below the coarse layer sediments are composed primarily of silts, fine sands, and organic materials, including roots, rootlets, and decaying matter. A return to this fine-grained sediment was observed in the top 1–2 mm of each core. Further below the fine-grained sediment lies fine-coarse sands.

Percent inorganic content was analyzed for each core and ranges between 94%–98% in the coarse grained layer (Figs. 7–9) with the finer-grained background sediments ranging between 87%–92%. A return to higher percent inorganic content (95%–98%) was observed in the deepest sediments. Percent moisture was lower in the coarser sediments, ranging from 22%–30%, and the finer-grained background sediments, ranging from 34%–50%. Grain size analyses indicate a fine-coarse sand grain size in the coarse layer, where all cores show a substantial percentage (>50%) of grains greater than 125 μm. Core BH1 yielded the largest range of grain size in this layer, ranging from 69%–91% grain size larger than 125 μm, with an average of 80% grain size above 125 μm (Fig. 7). Core BH2 showed a range of 47%–66% of grain size larger than 125 μm, averaging 56.5% (Fig. 8). Core BH3 showed ranges from 76%–95% of 125 μm grain size, with an average of 85.5% of the grains larger than 125 μm (Fig. 9).

4.3. Foraminifera assemblages of cores

Examination of the coarse-grained layer in all cores yielded several different foraminifera species (Table 1). Genera found included

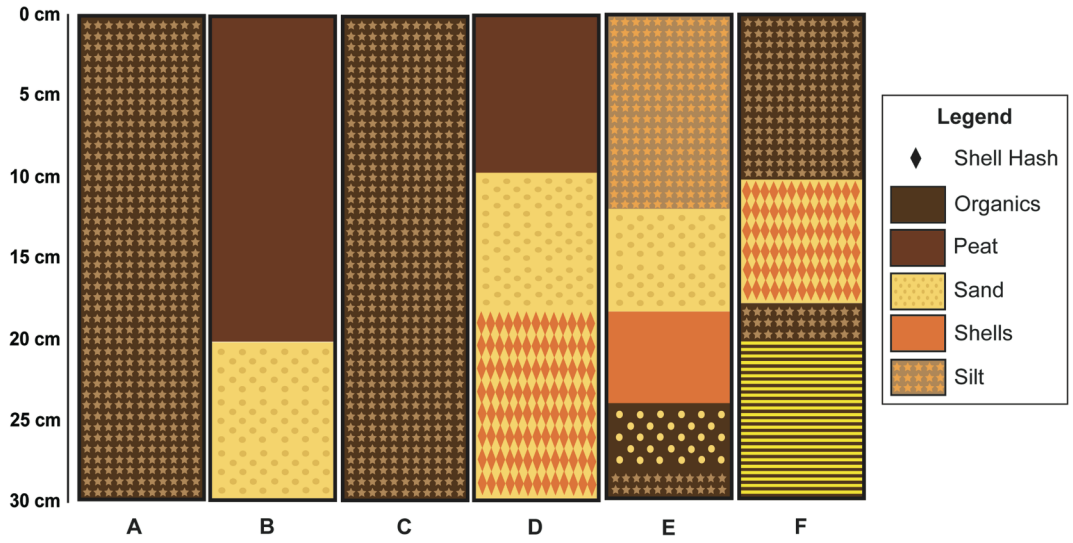

Fig. 3. Stratigraphic plots for cores A) Fishtrap Bay, B) North Lovers Key Lagoon, C) Mound Key Entrance, D) Imperial River Offshoot, E) Spring Creek, and F) Stingray Key.

Fig. 4. Core photographs for cores A) Fishtrap Bay, B) North Lovers Key Lagoon, C) Mound Key Entrance, D) Imperial River Offshoot, E) Spring Creek, and F) Stingray Key.

Ammonia, *Elphidium*, *Haynesina*, and *Quinqueloculina*. The entire sample from core BH3 was picked, whereas four subsamples of core BH1 and eight subsamples of core BH2 were collected. All picked forams were identified to the species level. *Ammonia tepida* was the most abundant species in all cores and *Quinqueloculina bosciana* was the least dominant. *Ammonia tepida* counts for cores BH1, BH2, and BH3 were 154, 200, and 158, respectively. Additionally, core BH2 had 152 *Elphidium galvestonense* individuals. *A. beccarii*, *Haynesina germanica*, and *Quinqueloculina bosciana* were also found in all the cores, but in lesser amounts. In total, 958 forams were picked for this study. *Ammonia* had the highest overall proportion of specimens at 60.75%, followed by *Elphidium* with 26.2%, *Haynesina* at 8.77%, and *Quinqueloculina* with 4.28%. In core BH1, *Ammonia tepida* comprised 63.37% of the total specimens picked whereas *Elphidium galvestonense* comprised 21.4%. In

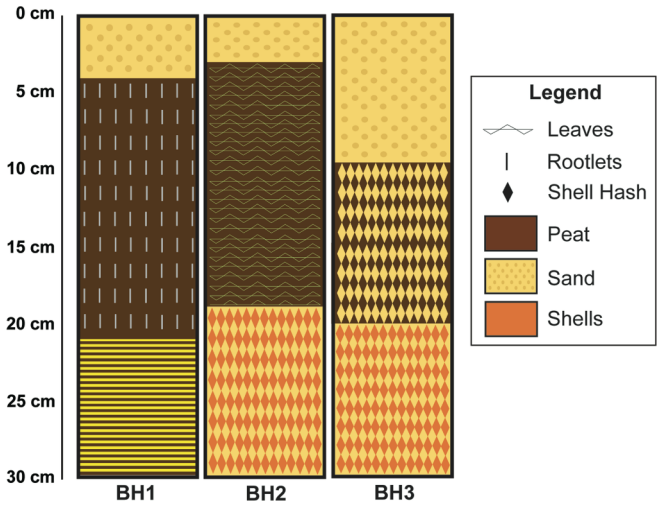

Fig. 5. Stratigraphic plots for cores BH1, BH2, and BH3. The tempestite layer was composed of medium to coarse-grained sand with small amounts (<5%) of calcareous shell hash.

core BH2, *Ammonia tepida* comprised 51.02% of the total specimens picked whereas *Elphidium galvestonense* comprised 38.78%. In core BH3, *Ammonia tepida* comprised 48.92% of the total specimens picked. Core BH3 was the only core where *Elphidium galvestonense* was not the second most dominant species, but instead *Haynesina germanica* was at 16.72%.

4.4. Core chronology

Excess ^{210}Pb concentrations in core BH4 are relatively low, ranging between 0.074 and 1.102 dpm/g (Table 2). The sediment core was dated using a CRS model. The CRS model assumes a constant rate of supply of atmospheric ^{210}Pb and allows variable sedimentation rates over time. Thus, it can be more applicable for shallow Southwest Florida coastal-marine environments where large anthropogenic activities alter the sediment loads (Appleby and Oldfield, 1992; Lubis, 2013; Adhikari et al., 2016). Errors represent counting statistics and were propagated following the method described by Binford (1990) (Table 2). The propagated errors vary between 7 and 13%. The CRS model for core BH4 (Table 2 and Fig. 10) indicates that sedimentation rates below 5 cm (5–20 cm) are 0.02–0.04 cm/yr and increase in the top 5 cm to 0.09–0.79 cm/yr.

5. Discussion

5.1. Estero Bay cores

Post Hurricane Irma cores were taken at seven Estero Bay sites (Fig. 1C) within a month of Irma's landfall. All these sites showed evidence of historic tempestites further downcore (20 cm or deeper) but no discernable evidence of recent storm activity, except for the tempestite located in the top sediments of the Big Hickory Island Lagoon (Fig. 1, yellow star). Hurricane Irma was a category 2 storm when it moved through Estero Bay, with a maximum recorded storm surge of 1.18 m, well below the expected 3.66 m minimum storm surge predicted by the National Hurricane Center (Cangialosi et al., 2018). Interestingly, prior to the arrival of the storm surge Estero Bay almost entirely emptied but refilled rapidly during the arrival of the surge (tide rising about 1.68 m/h; Cappucci, 2017). The 6 cores taken at sites Fishtrap Bay, North Lovers Key Lagoon, Mound Key Entrance, Imperial River Offshoot, Spring Creek and Stingray Key are all connected to Estero Bay proper (Fig. 1C). The absence of Hurricane Irma overwash at these sites was most likely due to their more protected locations. Sites close to the inner-bay margin such as Imperial River Offshoot, Spring Creek and Stingray Key are not only protected by fringing mangrove islands but are also located far from the barrier islands and their respective inlets. To transport overwash material this far into the bay significant storm surge energy would be required. Overwash material was also absent at sites Fishtrap Bay, North Lovers Key Lagoon and Mound Key Entrance. While these sites are closer to the Estero Bay barrier islands and their inlets, all three sites are considerably more protected from the Gulf of Mexico than the Big Hickory Island Lagoon. The overwash signatures found in the Big Hickory Island Lagoon are discussed below.

5.2. Core chronology at Big Hickory

^{210}Pb sediment dating in the Southwest Florida region can sometimes present challenges. Radionuclides such as ^{210}Pb adsorb more readily to organic-rich fine particles with higher surface areas, leading to higher accumulation rates in sediments that have higher percentages of fine-grained particles (Singleton et al., 2017). Unfortunately, sediments in coastal Southwest Florida environments are often quartz silt and sand-sized sediments, and, therefore, activities of excess ^{210}Pb tend to be relatively low (even after running samples for ~3 days on a high efficiency detector). Previous studies have reported low excess ^{210}Pb in Southwest Florida sediments (Trefry et al., 2004). Sediment composition, grain size, and the lower sedimentation rates present a challenge in Southwest Florida, unlike other areas along the northern Gulf of Mexico, such as the Mississippi River delta (Trefry et al., 2004). Despite these challenges, core dating from Big Hickory Island Lagoon was accomplished (Table 2).

Excess ^{210}Pb concentrations in core BH4 are relatively low (Table 2), as seen in other studies (Trefry et al., 2004), and that downcore trends in excess ^{210}Pb concentrations do not follow a traditional downcore ^{210}Pb decay profile. This could be an artifact of the relatively high calculated errors on samples with low concentrations. It could also be due to very high accumulation rates in the core top, caused by a pulse deposition due to storm activity and the subsequent dilution of excess ^{210}Pb. Another possible explanation for this is a result of sediment mixing. Because Irma occurred in 2017, this study is most concerned with constraining the core tops (~0–5 cm). Therefore, even though the ^{210}Pb may not look like a traditional ^{210}Pb decay profile, perhaps due to the one or more of the factors listed above, the upper 0–5 cm most likely represent the last ~11 ± 1.4 years calculated by the Constant Rate of Supply (CRS) model. The CRS model indicates high sedimentation rates in the top 5 cm to 0.09–0.79 cm/yr, which would be in alignment with a pulse sediment depositional event. Below 5 cm (5–12 cm) sedimentation rates are 0.02–0.04 cm/yr (Fig. 10), which is in alignment with previous studies in the Estero Bay area (Trefry et al., 2004) that showed similar sedimentation rates.

5.3. Interpretation of sediment record at Big Hickory

Two interpretations can be made from Big Hickory Island Lagoon sediment cores. First, there is an overall slow change from an open bay setting to the closed lagoon that is present today. The fine-coarse, poorly sorted sands present in the bottom of the cores are characteristic of an open bay setting. Using the ^{210}Pb dating it is estimated that sometime in the early 1900s the bay closed off allowing for the deposition of the lagoonal sediments that are observed in the upper sections of the Big Hickory Island Lagoon cores. These undisturbed silts, fine sands, and organic materials – including roots, rootlets, and decaying matter – are indicative of a low energy lagoonal setting. The sediments observed in the core tops are also indicative of the modern low energy depositional setting of the lagoon, indiating that normal deposition resumed after the passing of Hurricane Irma. Secondly, the Big Hickory Island Lagoon cores are all perturbed by a high-energy event in the very upper sediments (BH1 = 4.0 cm, BH2 = 3.0 cm, BH3 = 9.5 cm, BH4 = 2.0 cm) (Fig. 5). Because low-energy lagoonal sediments are present both below and above this high-energy event layer this layer has been interpreted as

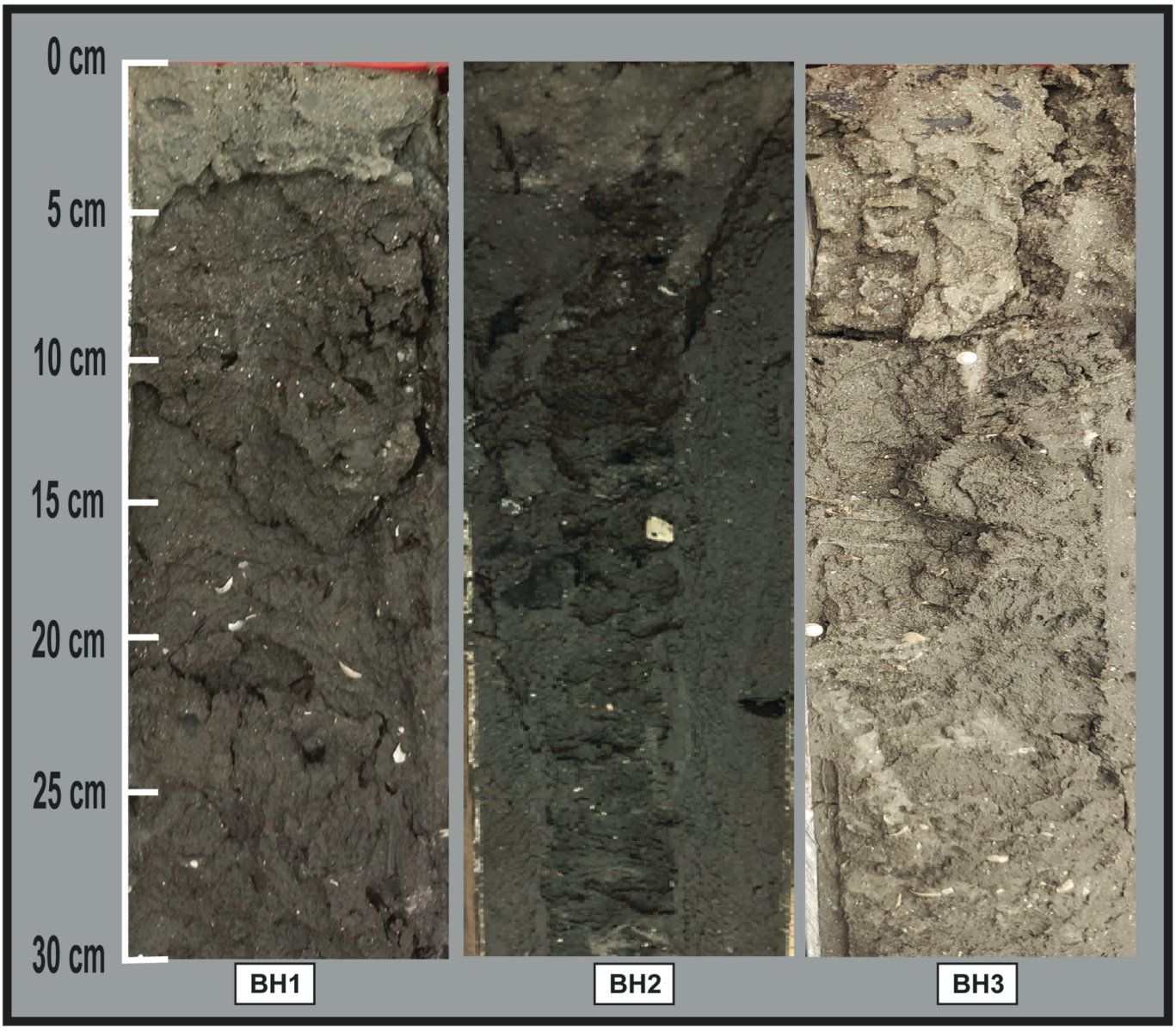

Fig. 6. Core photographs for cores BH1, BH2, and BH3.

a storm-induced tempestite. Using the ^{210}Pb dating it is estimated that this tempestite was deposited during the landfall of Hurricane Irma in 2017. This interpretation is also supported by previous cores taken at this site (pre-2017) that do not contain a tempestite in the upper sediments.

The presence of foraminifera species in the tempestite layer indicates that the sediment deposited in the lagoon was of marine origin. All species found have a wide geographic distribution that includes the Gulf of Mexico (Ishman, 2000), some of which are shallow organisms and some of which are deep sea organisms. *Ammonia tepida* are benthic foraminifera commonly found in brackish environments with salinity less than 33‰ (Debenay et al., 1998), but can be found in marine environments with a higher salinity. They live in epipelic or shallow endopelic environments (in or on sediments) often made of fine sand (Debenay et al., 1998). In other words, it is possible that the high abundance of this species in these core samples can be attributed to the many barrier beach migrations and shoreline changes (Briggs and Elko, 2016) that Big Hickory Island has undergone since formation. *A. beccarii* are shallow-living marine foraminifera that live in salinity greater than 33‰ (Gonzalez, 1998). They are also epipelic or endopelic, but in coarser sands. These foraminifera most likely came from the Gulf of Mexico and were deposited by Hurricane Irma's storm surge. *Elphidium galvestonense* is a benthic marine foraminifera species that is abundant in the shallow waters of the Gulf of Mexico where the chlorinity ranges from 5 to 15‰ (Ishman, 2000). *Haynesina germanica* are dominant in intertidal coastal areas at salinities greater than 18‰ (Ishman, 2000). *Quinqueloculina bosciana* is a benthic species that lives in open bay coarse sediments and where there is seagrass coverage (Stone et al., 2000). No foraminifera were found in the closed lagoonal sediments present below the tempestites. A subsample from two different intervals was studied for the closed lagoonal sediments (11–12 cm and 18–19 cm) of each core. The absence of foraminifera in these sediments indicate that no marine influence occurred at the time of deposition. The presence of several different marine foraminifera species in the tempestite samples, coupled with the absence of foraminifera in the closed lagoonal sediments, displays the ability of Hurricane Irma's storm surge to overcome coastal barrier landforms and deposit marine sediments in the back-barrier lagoon. Results of this study indicate that tempestite thickness may be a function of the width of the beach. The tempestites for cores BH1 and BH2 were 4.0 cm and 3.0 cm, respectively, whereas core BH3

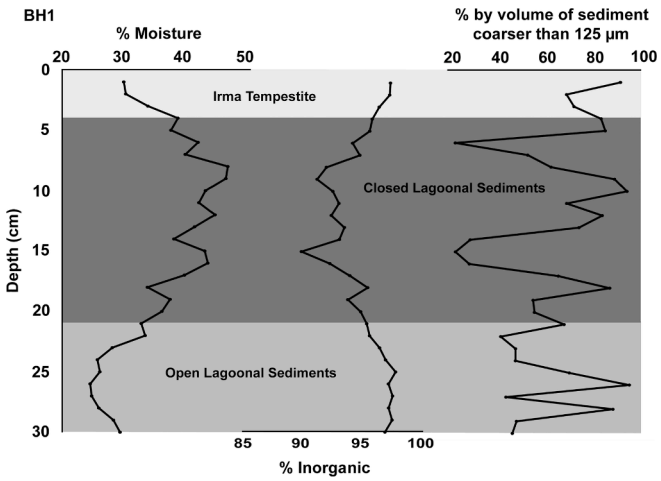

Fig. 7. Sediment proxies for core BH1. Gray bands indicate differing environments within the core, with the top being the tempestite deposited by Hurricane Irma, followed by closed lagoonal sediments and open lagoonal sediments. Grain size was determined by the percent volume of sediment coarser than 125 μm. Larger grain size, low moisture content, and high inorganic content are indicative of the tempestite layer.

was 9.5 cm. Core BH3 was taken in the portion of the lagoon perpendicular the shortest beach length (Fig. 2). BP2 indicates that dune height in this transect is slightly higher (~0.88 m) than the dune in front of cores BH1 and BH2 (0.83 m). Core BH2 contained the thinnest tempestite and was taken directly behind a wider section of the barrier (BP1). It has been recognized in previous studies that alongshore variations in dune height and width direct barrier island response to storm surge (Houser et al., 2008; Houser et al., 2018). This study supports early work that demonstrates that beach width is important for overwash deposition.

Core stratigraphy indicates that the storm surge produced by Hurricane Irma likely deposited a tempestite at this site in Sallenger's (2000) Overwash Regime, which is the second strongest storm surge regime. The storm surge and waves in this regime overtop the dunes and begin the process of overwash (Sallenger, 2000). The sand from this overwash is then redeposited landward where it remains (Sallenger, 2000). This is consistent with the sedimentology being mostly fine-medium grained sands, rather than the coarse-grained sands and shell hash you might expect during the Inundation Regime (Sallenger, 2000).

Evidence of additional tempestites downcore do not exist in the Big Hickory Island Lagoon cores, even though this region was impacted by intense storms in the modern day, such as Hurricane Donna in 1960 (~3.35 m storm surge in Naples, FL). This may be explained by the extra protection from an additional barrier island seaward of the present-day foreshore that is noted in historic aerial images (discussed below in detail in Section 5.3) between 1944 and 1958 (Fig. 11). The additional barrier island may have offered protection from past intense hurricanes, such as Hurricane Donna. However, the present-day geomorphology of the single barrier (narrow and low in elevation) allowed Hurricane Irma to overwash the present-day barrier and deposit a tempestite. This further supports the theory that barrier islands are crucial in protecting the environments behind them (Irish et al., 2010).

5.4. Storm history and past barrier storm response

Southwest Florida barrier islands tend to have low elevation and Big Hickory Island is no exception (present day <0.9 m), creating a susceptibility to the Overwash and Inundation regimes. In the beach profiles two main changes are of note. First, substantial erosion reduced the overall height of the beach profile from 1.5 m in 2015 to 0.88 m in 2018 (Fig. 2). It is likely that Hurricane Irma in 2017 had a significant erosive

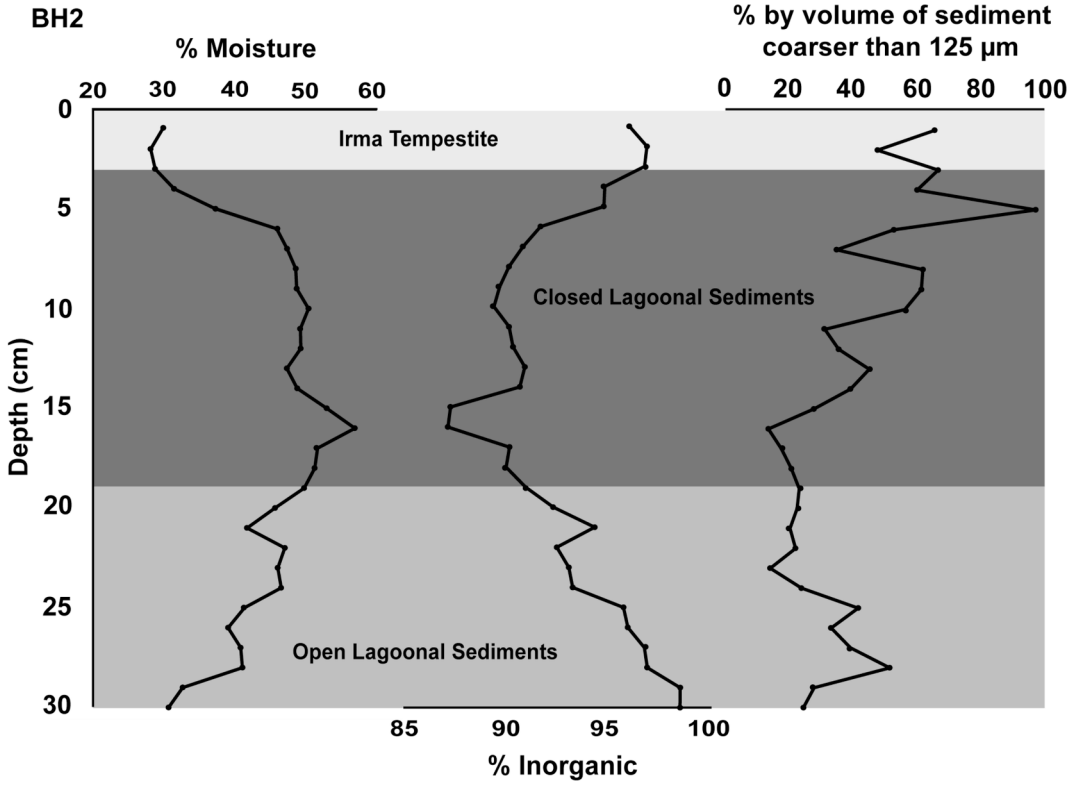

Fig. 8. Sediment proxies for core BH2. Gray bands indicate differing environments within the core, with the top being the tempestite deposited by Hurricane Irma, followed by closed lagoonal sediments and open lagoonal sediments. Grain size was determined by the percent volume of sediment coarser than 125 μm. Larger grain size, low moisture content, and high inorganic content are indicative of the tempestite layer.

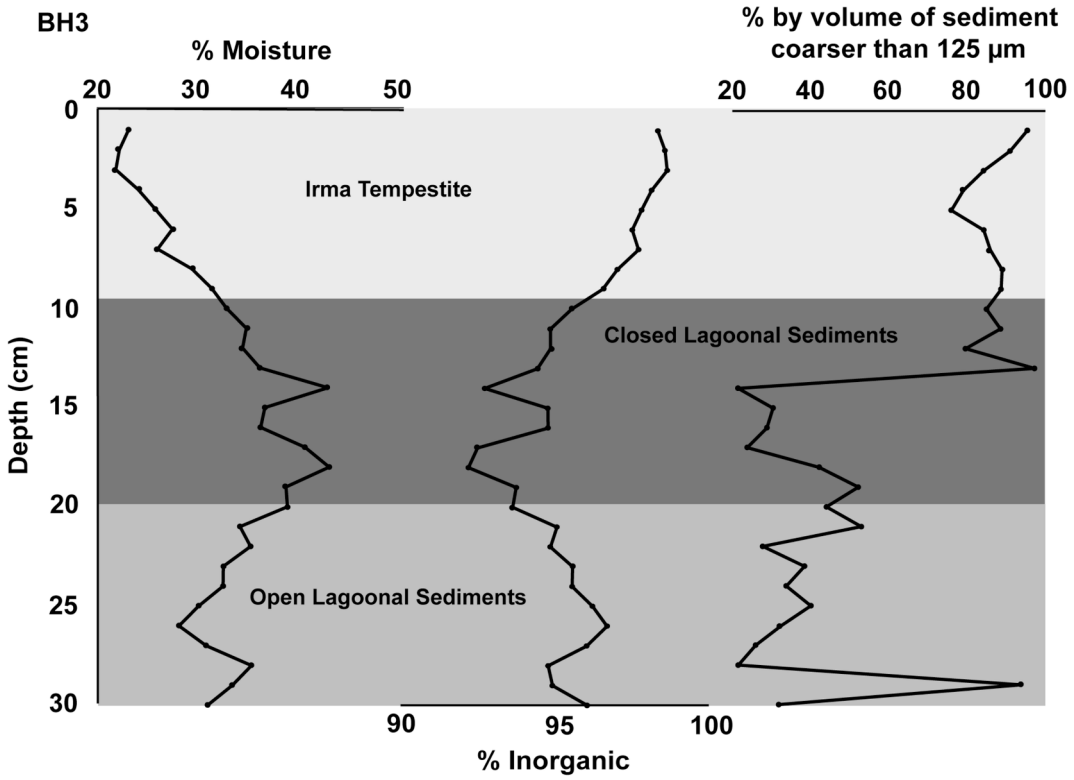

Fig. 9. Sediment proxies for core BH3. Gray bands indicate differing environments within the core, with the top being the tempestite deposited by Hurricane Irma, followed by closed lagoonal sediments and open lagoonal sediments. Grain size was determined by the percent volume of sediment coarser than 125 μm. Larger grain size, low moisture content, and high inorganic content are indicative of the tempestite layer.

Table 1
Individual foraminifera count for each core. Foraminifera were only found in the tempestite, not in the lagoonal sediments. *Ammonia tepida* was the dominant species in all cores, and *Quinqueloculina bosciana* was the least dominant. % abundance was determined from the number of a species divided by the total number of specimens for each core.

Individuals counted				% Abundance			
Species	BH1	BH2	BH3	Species	BH1	BH2	BH3
Ammonia tepida	154	200	158	*Ammonia tepida*	63.37	51.02	48.92
Ammonia beccarii	17	22	31	*Ammonia beccarii*	7.00	5.61	9.60
Elphidium galvestonense	52	152	47	*Elphidium galvestonense*	21.40	38.78	14.55
Haynesina germanica	14	16	54	*Haynesina germanica*	5.76	4.08	16.72
Quinqueloculina bosciana	6	2	33	*Quinqueloculina bosciana*	2.47	0.51	10.22

Table 2
Sediment analyses for Excess ^{210}Pb (dpm/g). Sediment ages were calculated based on the Constant Rate of Supply (CRS) Model (Binford, 1990).

Depth (cm)	Excess 210Pb (dpm/g)	Dry density of sed. (g/cc)	CRS estimated time (yr)	CRS propagated error (%)	Error (±yr)	Sed. rate (cm/yr)
0–0.5	0.477	1.003	0.6	12.290	0.1	0.787
0.5–1.0	0.671	1.228	1.8	9.800	0.2	0.284
10–1.5	0.734	1.397	3.2	8.910	0.3	0.155
1.5–2.0	0.768	1.234	4.6	9.680	0.4	0.108
2.0–3.0	1.102	1.027	8.3	7.730	0.6	0.121
4.0–5.0	0.074	1.470	11.1	12.320	1.4	0.090
5.5–6.0	0.493	3.072	15.7	9.970	1.6	0.032
6.5–7.0	0.134	1.317	16.9	11.820	2.0	0.030
7.5–8.0	0.164	1.643	18.2	9.870	1.8	0.027
8.5–9.0	0.900	2.881	26.9	7.910	2.1	0.019
9.5–10.0	0.216	1.438	31.5	9.660	3.0	0.016
11.0–12.0	0.434	2.194	43.3	9.070	3.9	0.023

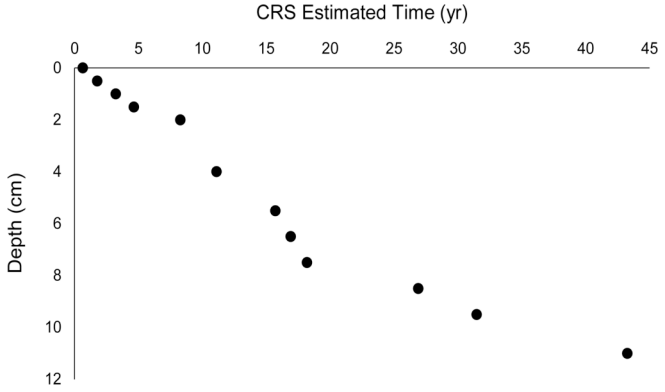

Fig. 10. Calculated sediment ages, based on the Constant Rate of Supply (CRS) Model (Binford, 1990).

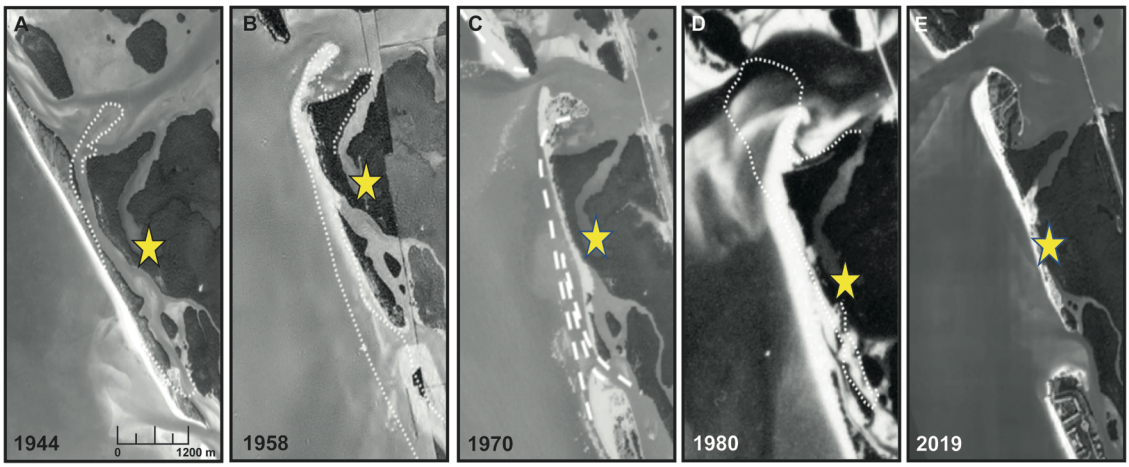

Fig. 11. Historical satellite images of Big Hickory Barrier Island. The yellow star indicates The Big Hickory Island Lagoon. A) 1944 aerial photograph with the approximate 1958 shoreline shown as a white dashed line. B) 1958 aerial photograph with the approximate 1980 shoreline shown as a white dashed line. C) 1970 aerial photograph with the approximate 1980 shoreline shown as a white dashed line. D) 1980 aerial photograph with the approximate 1996 shoreline shown as a white dashed line. Images A, B, C, and D are adapted from Briggs and Elko, 2016. E) The most recent aerial photograph was sourced from Google Earth. (For interpretation of the references to colour in this figure legend, the reader is referred to the web version of this article.)

effect on this segment of beach. USGS storm tide sensors in Naples and at Delnor-Wiggins State Park near Naples Park measured water levels of 1.54 m NAVD88 (1.37 m MHHW) and 1.19 m NAVD88 (1.04 m MHHW) (Cangialosi et al., 2018). Secondly, the beach profiles indicate a landward migration of the foreshore and dune. This is also an indication of Overwash Regime where the landward transport of sediment can lead to a migration of the barrier over time (Sallenger, 2000).

Historic satellite imagery demonstrates the dynamic nature of the Big Hickory Barrier Island prior to Hurricane Irma (Figs. 11 and 12). Fig. 11 shows a series of historic satellite images of Big Hickory Island from 1944, 1958, 1970, 1980 and 2019. As noted by Briggs and Elko (2016) historic images demonstrate high long-term rates of shoreline recession and a landward migration of the Big Hickory Barrier Island through time. What is most notable is the almost complete disappearance of a separate barrier, that was once seaward of the current barrier island foreshore, between 1944 and 1958. The 1947 Fort Lauderdale hurricane may have been responsible for some of this erosion as it produced sustained winds of 190 km/h at the Sanibel Island Lighthouse (Sumner, 1947), inundation of 0.91 m at the Sanibel Island coast guard station and peak tides at Everglades City of 1.7 m (Barnes, 1998).

Substantial erosion and landward movement of the barrier was also noted between 1958 and 1970. This period saw the passing of Hurricane Donna, the most significant hurricane to have made impact in this region during modern historical time. Hurricane Donna made direct landfall in Naples, Florida as a Category 4 storm in 1960. This storm was responsible for >3.35 m of storm surge and 0.3 m of rain in Southwest Florida as well as ~$387 to $426 million in damages nationwide at the time (Dunn, 1961; Sugg et al., 1971). Wind gusts up to 185 km/h were recorded in Fort Myers, with tides of 3.11 m at nearby Estero Island and Naples (Dunn, 1961; Sugg et al., 1971). Between 1970 and 1980 there appears to be some accretion along the Big Hickory Barrier Island dune and foreshore complex. No significant storms of note made landfall during this period, besides an unnamed tropical depression in 1971. If hurricanes are a significant factor in coastal erosion processes, then this would explain why these years saw lower erosion rates than the previous years.

Satellite imagery from 1994 shows that the Big Hickory Island Lagoon was once connected to Estero Bay (Fig. 12A). During this period there was a well-developed mangrove forest between the lagoon and the dune/foreshore. Between 1994 and 2005 the presence of overwash fans into the lagoon can be observed. The 2004 season experienced the landfall of Hurricane Charlie on Captiva Island, just 55 km north of Big

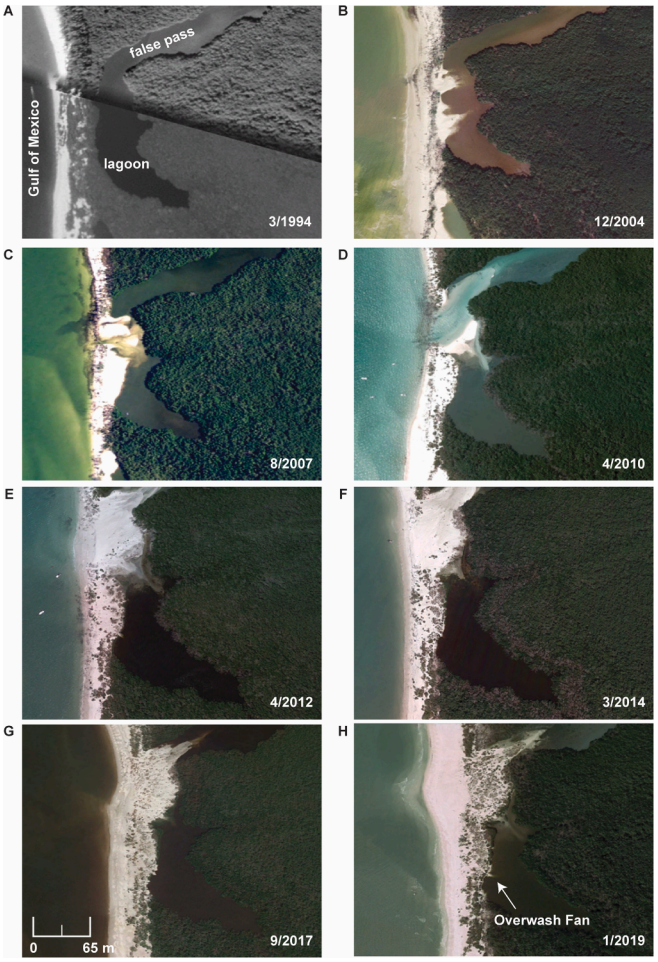

Fig. 12. Satellite photographs of the study site showing the dynamic nature of the lagoon. Photographs were taken in A) March 1994; B) December 2004; C) August 2007; D) April 2010; E) April 2012; F) March 2014; G) September 2017; and H) January 2019. Images courtesy of Google Earth.

Hickory Island, and 2005 saw the landfall of Hurricane Wilma at Cape Romano, just 71 km south of Big Hickory Island. Hurricane Charley was a Category 4 hurricane, but due to its small size it was mostly a wind event (183 km/h winds but only within the 10-km radius eye wall) with a relatively small storm surge of ~1.33 m (Wang et al., 2005). Hurricane Wilma was a Category 3 hurricane (185 km/h winds within the 137-km radius) also with a relatively small storm surge of ~0.9 m in Naples (Byrne, 2006). It is possible that the combination of hurricanes Charley and Wilma was responsible for some of the mangrove loss along this portion of Big Hickory Barrier Island – from wind and inundation. It is likely that the overwash fans observed in Fig. 12B were a result of Hurricane Charley, since the ~1.33 m storm surge most likely overtopped the barrier dune system of ~0.9 m.

By August 2007, these overwash fans had begun to close the lagoon off from Estero Bay and between August 2007 and December 2008 even more deposition took place to further isolate the lagoon from Estero Bay. By December 2009, the small tidal inlet north of the lagoon was open to the Gulf of Mexico and remained open until at least April 2010. Though the lagoon itself was still closed to the Gulf of Mexico during this time, the aerial photography sequence indicates that this was a significant erosional period. However, there were no intense hurricanes making landfall in this region between December 2008 and December 2009. The only storm that impacted Southwest Florida in 2009 was Tropical Storm Claudette, which formed offshore in the Gulf of Mexico (Berg and Avila, 2010). By 2012 the small inlet was closed again, and the lagoon was separated from the Gulf of Mexico and the inlet. From 2009 to 2012 very few storms impacted Southwest Florida and it appears that this was largely a period of deposition. Tropical Storm Bonnie (2010) was a small and rather weak tropical storm that made landfall in Southwest Florida as a back-door storm, likely having little impact on beach erosion.

In 2013, ~86,300 m^3 of sand from a tidal inlet to the north were artificially placed as nourishment along 457 m of the island to restore the beach and dune system. In addition, seven concrete king-pile groins with adjustable panels were constructed after the completion of the beach nourishment. The addition of this sand to the south of the study site and therefore subsequent replenishment of the foreshore and dune is evident in the 2014, 2017, and 2019 aerial images. The lagoon has remained closed to present day, which is also evidenced in the lagoonal sediments as being largely organic in nature (top 19–21 cm) (Figs. 7–9). Between 2017 and 2018 a small overwash fan can be observed toward the middle of the lagoon which was most likely deposited by Hurricane Irma in September of 2017 (Fig. 12H). This overwash fan, which was used as reference point for collecting the cores, is discussed below. The above storm history, paired with the geomorphological changes to the Big Hickory Barrier through time, indicates the strong association between storm activity and barrier island erosion.

5.5. *Implications for Paleo storm record reconstruction along Barrier Coast*

Storm surge from Hurricane Irma in 2017 deposited sediment into the Big Hickory back-barrier lagoon due to the shallow and narrow dune and foreshore. Irma's tempestite layers were thicker behind narrower beach sections, indicating the importance of foreshore/dune height and width. This is supported by previous studies from Houser et al. (2008) demonstrating that narrow beaches with no dune development tend to undergo more overwash penetration and island breaching. In contrast, wider sections of beach with large foredunes and back-barrier dunes experience less overwash penetration (Houser et al., 2008).

Hurricane Irma was able to overwash the Big Hickory Barrier Island foreshore and dune, whereas previous hurricanes were not, due to additional offshore barrier islands that once existed (1944 to 1958; Fig. 11). This research highlights the importance of barrier island geomorphology in interpreting paleotempestology records from back-barrier lagoons. Since barriers are so susceptible to processes of erosion and accretion care must be taken when interpreting the stratigraphic record of back-barrier cores, especially those situated in locations with dynamic recent histories, such as the Big Hickory Island Complex. These concerns have been discussed in previous studies, such as Hippensteel et al. (2013), and call for caution in the interpretation of paleotempestology from back-barrier settings. This work also calls for an overall better understanding of hurricane deposition and preservation in marginal-marine environments (Hippensteel et al., 2013).

6. Conclusion

Through the combination of historic satellite images, core sedimentology and radiometric dating, this study examines the history of the Big Hickory Lagoon and Island. Sediments at the base of the lagoonal cores indicate an open bay setting, seen in previous studies from Estero Bay (Wohlpart et al., 2007) that indicate a past connection between Estero Bay and the Gulf of Mexico. Lagoonal sediments dominate the middle section of the cores, overlain by an inorganic layer of fine to medium-grained marine sand (tempestite) deposited during the passing of Hurricane Irma in 2017. It is likely that Hurricane Irma reached the Overwash Regime (Sallenger, 2000) and deposited sand from the beach and dunes into the lagoon. Evidence of Hurricane Irma is not found in any other Estero Bay field sites demonstrating that hurricanes with greater storm surge intensity are required to deposit overwash sediments into Estero Bay proper.

Historic aerial imagery and beach profiles demonstrate Big Hickory Island as a dynamic environment, susceptible to rapid geomorphological change through time. It is likely that historic storms have had a significant erosive effect on the barrier island over the past 76 years, as previously noted by Briggs and Elko (2016). Between 1944 and 1958 the island had extra protection from storm damage due to an additional barrier seaward of the present-day foreshore. Today this offshore barrier does not exist, most likely due to the erosive power of Hurricane Donna (1960) and other historic storms. As hurricanes continue to strengthen, due to current and projected atmospheric and oceanic warming (Emanuel, 2005), hurricane overwash events will become more prevalent. This makes barrier islands extremely vulnerable landscapes in the future. Understanding geomorphologic change of Southwest Florida barrier islands through time and their response to hurricane events will be particularly important for coastal managers. More specifically, understanding potential areas of overwash and erosion vulnerability will be crucial for future decisions around coastal resilience and infrastructure planning.

Funding sources

Funding for this project was provided by the National Science Foundation (OCE-1335375; OCE-1335207; OCE-1919813) and The Southwest Florida Community Foundation (55462).

Data availability

All data collected from the cores in this study are discussed and shown in the article. All core datasets have been uploaded to Mendeley Data and can be found at doi.10.17632/2gzs93xgv6.1.

Declaration of Competing Interest

The authors declare that they have no known competing financial interests or personal relationships that could have appeared to influence the work reported in this paper.

Acknowledgments

We would like to thank all of those who helped with the collection and analysis of data for this project. Thanks to Nick Culligan, Cody Calandra, Lexxi Morales, and Adam Catasus for assistance with

collecting cores. Thanks to Dr. Felix Jose and Andrew Gross for assisting with LiDAR and profile mapping data. Thanks to Dr. Puspa Adhikari and LSU for ^{210}Pb dating of cores. We would also like to thank two reviewers that provided extremely helpful reviews.

References

Adhikari, P.L., Maiti, K., Overton, E.B., Rosenheim, B.E., Marx, B.D., 2016. Distributions and accumulation rates of polycyclic aromatic hydrocarbons in the northern Gulf of Mexico sediments. Environ. Pollut. 212, 413–423. https://doi.org/10.1016/j.envpol.2016.01.064.

Appleby, P.G., Oldfield, F., 1978. The calculation of lead-210 dates assuming a constant rate of supply of unsupported 210Pb to the sediment. Catena 5, 1–8.

Appleby, P.G., Oldfield, F., 1983. The assessment of 210 Pb data from sites with varying sediment accumulation rates. Hydrobiologia 103 (1), 29–35.

Appleby, P.G., Oldfield, F., 1992. Applications of lead-210 to sedimentation studies. In: Uranium-Series Disequilibrium: Applications to Earth, Marine, and Environmental Sciences, 2 Ed.

Barnes, J., 1998. Florida's Hurricane History. UNC Press Books, ISBN 978-0807824436.

Berg, R., Avila, L., 2010. The 2009 Atlantic hurricane season: a slow summer, quiet fall. Weatherwise: The Power, The Beauty, The Excitement 63 (3), 42–49. https://doi.org/10.1080/00431671003733034.

Binford, M.W., 1990. Calculation and uncertainty analysis of 210Pb dates for PIRLA project lake sediment cores. J. Paleolimnol. 3 (3), 253–267. https://doi.org/10.1007/BF00219461.

Binford, M.W., Brenner, M., 1986. Dilution of 210Pb by organic sedimentation in lakes of different trophic states, and application to studies of sediment-water interactions 1. Limnol. Oceanogr. 31 (3), 584–595.

Briggs, T.M.R., Elko, N., 2016. Natural and human-induced dynamics on Big Hickory Island, Florida. J. Mar. Sci. Eng. 4 (1), 14. https://doi.org/10.3390/jmse4010014.

Buynevich, I.V., Donnelly, J.P., 2006. Geological signatures of barrier breaching and overwash, southern Massachusetts, U.S.A. J. Coast. Res. SI 39, 112–116. https://doi.org/10.2112/JCOASTRES-D-14-00109.1.

Buynevich, I.V., FitzGerald, D.M., van Heteren, S., 2004. Sedimentary records of intense storms in Holocene barrier sequences, Maine, USA. Mar. Geol. 210, 135–148. https://doi.org/10.1016/j.margeo.2004.05.007.

Byrne, M., 2006. Monitoring Hurricane Wilma's storm surge. In: USGS Sound Waves Newsletter. Retrieved from. https://archive.usgs.gov/archive/sites/soundwaves.usgs.gov/2006/02/index.html.

Byrne, M.J., Gabaldon, J.N., 2008. Hydrodynamic characteristics and salinity patterns in Estero Bay, Lee County, Florida. In: *U.S.* Geological Survey Scientific Investigations Report. https://doi.org/10.3133/sir20075217.

Cangialosi, J.P., Latto, A.S., Berg, R., 2018. National Hurricane Center Tropical Cyclone Report: Hurricane Irma. Retrieved from. https://www.nhc.noaa.gov/data/tcr/AL112017_Irma.pdf.

Cappucci, M., 2017. Hurricane Irma drained the water from Florida's biggest bays-but it wasn't gone for long. The Washington Post. Retrieved from. https://www.washingtonpost.com/news/capital-weather-gang/wp/2017/09/11/hurricane-irma-drained-the-water-from-floridas-largest-bays-but-it-wasnt-gone-for-long/.

Congressional Budget Office, 2019. Expected Costs of Damage from Hurricane Winds and Storm-Related Flooding. Retrieved from. https://www.cbo.gov/system/files/2019-04/55019-ExpectedCostsFromWindStorm.pdf.

Debenay, J.P., Bénéteau, E., Zhang, J., Stouff, V., Geslin, E., Redois, F., Fernandez-Gonzalez, M., 1998. *Ammonia beccarii* and *Ammonia tepida* (foraminifera): morphofunctional arguments for their distinction. Mar. Micropaleontol. 34 (3–4), 235–244.

Diaz, H.F., Pulwarty, R.S. (Eds.), 1997. Hurricanes: Climate and Socioeconomic Impacts. Springer Science & Business. https://doi.org/10.1007/978-3-642-60672-4.

Donnelly, J.P., Roll, S., Wengren, M., Butler, J., Lederer, R., Webb III, T., 2001. Sedimentary evidence of intense hurricane strikes from New Jersey. Geology 29, 615–618. https://doi.org/10.1130/0091-7613(2001)029<0615:SEOIHS>2.0.CO;2.

Donnelly, J.P., Butler, J., Roll, S., Wengren, M., Webb III, T., 2004. A backbarrier overwash record of intense storms from Brigantine, New Jersey. Mar. Geol. 210, 107–121. https://doi.org/10.1016/j.margeo.2004.05.005.

Dunn, G.E., 1961. The hurricane season of 1960. Mon. Weather Rev. 89 (3), 99–108. https://doi.org/10.1080/00431672.1961.9933185.

Emanuel, K., 2005. Increasing destructiveness of tropical cyclones over the past 30 years. Nature 436, 686–688. https://doi.org/10.1038/nature03906.

Ercolani, C., Muller, J., Collins, J., Savarese, M., Squiccimara, L., 2015. Intense Southwest Florida hurricane landfalls over the past 1000 years. Quat. Sci. Rev. 126, 17–25. https://doi.org/10.1016/j.quascirev.2015.08.008.

Florida Department of Environmental Protection, 2018. Hurricane Irma Post-Storm Beach Conditions and Coastal Impact in Florida. Retrieved from. https://floridadep.gov/rcp/coastal-engineering-geology/documents/hurricane-irma-post-storm-beach-conditions-and-coastal.

Ginsburg, R.N., Lloyd, R.M., 1956. A manual piston coring device for use in shallow water. J. Sediment. Res. 26, 64–66.

Halverson, J.B., 2018. The costliest hurricane season in U.S. history. Weatherwise 71 (2), 20–27. https://doi.org/10.1080/00431672.2018.1416862.

Hippensteel, S.P., Martin, R.E., 1999. Foraminifera as an indicator of overwash deposits, barrier island sediment supply, and barrier island evolution, Folly Island, South Carolina. Palaeogeogr. Palaeoclimatol. 149, 115–125. https://doi.org/10.1016/S0031-0182(98)00196-5.

Hippensteel, S.P., Eastin, M.D., Garcia, W.J., 2013. The geological legacy of Hurricane Irene: implications for the fidelity of the paleo-storm record. GSA Today 23 (12), 4–10.

Houser, C., Hapke, C., Hamilton, S., 2008. Controls on coastal dune morphology, shoreline erosion and barrier island response to extreme storms. Geomorphology 100, 223–240. https://doi.org/10.1016/j.geomorph.2007.12.007.

Houser, C., Wernette, P., Weymer, B., 2018. Scale dependent behavior the foredune: Implications for barrier island response to storms and sea level rise. Geomorphology 303, 362–374. https://doi.org/10.1016/j.geomorph.2017.12.011.

Irish, L., Freya, A.E., Rosati, J.D., Olivera, F., Dunkin, L.M., Kaihatu, J.M., Ferreira, C.M., Edge, B.L., 2010. Potential implications of global warming and barrier island degradation on future hurricane inundation, property damages, and population impacted. Ocean Coast. Manag. 53 (10), 645–657. https://doi.org/10.1016/j.ocecoaman.2010.08.001.

Ishman, S.E., 2000. Benthic foraminiferal distributions in South Florida. Top. Geobiol. Environ. Micropaleontol. 15, 371–383. https://doi.org/10.1007/978-1-4615-4167-7_17.

Jung, K., Shavitt, S., Viswanathan, M., Hilbe, J.M., 2014. Female hurricanes are deadlier than male hurricanes. Proc. Natl. Acad. Sci. 111 (24), 8782–8787. https://doi.org/10.1073/pnas.1402786111.

Klotzbach, P.J., Schreck III, C.J., Collins, J.M., Bell, M.M., Blake, E.S., Roache, D., 2018. The extremely active 2017 North Atlantic hurricane season. Mon. Weather Rev. 146, 3425–3443. https://doi.org/10.1175/MWR-D-18-0078.1.

Krishnaswamy, S., Lal, D., Martin, J.M., Meybeck, M., 1971. Geochronology of lake sediments. Earth Planet. Sci. Lett. 11 (1–5), 407–414.

Landsea, C.W., Hagen, A., Bredemeyer, W., Carrasco, C., Glenn, D.A., Santiago, A., Strahan-Sakoskie, D., Dickinson, M., 2014. A reanalysis of the 1931-43 Atlantic hurricane database. J. Clim. 27 (16), 6093–6118. https://doi.org/10.1175/JCLI-D-13-00503.1.

Lane, P., Donnelly, J.P., Woodruff, J.D., Hawkes, A.D., 2011. A decadally-resolved paleohurricane record archived in the late-Holocene sediments of a Florida sinkhole. Mar. Geol. 287, 14–30. https://doi.org/10.1016/j.margeo.2011.07.001.

Lin, N., Lane, P., Emanuel, K.A., Sullivan, R.M., Donnelly, J.P., 2014. Heightened hurricane surge risk in northwest Florida revealed from climatological-hydrodynamic modeling and paleorecord reconstruction. J. Geophys. Res. Atmos. 119 (14), 8606–8623. https://doi.org/10.1002/2014JD021584.

Liu, K.B., Fearn, M.L., 1993. Lake-sediment record of late Holocene hurricane activities from coastal Alabama. Geology 21 (9), 793–796. https://doi.org/10.1130/0091-7613(1994)022<0285:LSROLH>2.3.CO;2.

Liu, K.B., Fearn, M.L., 2000. Reconstruction of prehistoric landfall frequencies of catastrophic hurricanes in northwestern Florida from lake sediment records. Quat. Res. 54 (2), 238–245. https://doi.org/10.1006/qres.2000.2166.

Lubis, A.A., 2013. Constant rate of supply (CRS) model for determining the sediment accumulation rates in the coastal area using 210Pb. J. Coast. Dev. 10 (2013), 9–18.

McCloskey, T.A., Keller, G., 2009. 5000 year sedimentary record of hurricane strikes on the central coast of Belize. Quat. Int. 195 (1–2), 53–68. https://doi.org/10.1016/j.quaint.2008.03.003.

Nordhaus, W.D., 2010. The economics of hurricanes and implications of global warming. Clim. Chang. Econ. 1 (1), 1–20. https://doi.org/10.1142/S2010007810000054.

Obley, S.P., Savarese, M., Tedesco, L.P., 2001. The influence of sea level rise on the history of estuarine environments in Southwest Florida. In: 16th Biennial Conference of the Estuarine Research Federation. Abstract Volume, 102.

Plant, N.G., Stockdon, H.F., 2012. Probabilistic prediction of barrier-island response to hurricanes. J. Geophys. Res. Earth Surf. 117 (F3), 1–17. https://doi.org/10.1029/2011JF002326.

Risi, J.A., Wanless, H.R., Tedesco, L.P., Gelsanliter, S., 1995. Catastrophic sedimentation from Hurricane Andrew along the southwest Florida coast. J. Coast. Res. 83–102.

Sallenger, A.H., 2000. Storm impact scale for barrier islands. J. Coast. Res. 16 (3), 890–895.

Schwartz, R.K., 1975. Nature and genesis of some storm washover deposits. CERP Tech, p. 69. Memo no. 61. https://doi.org/10.13140/RG.2.1.2216.9449.

Scott, D.B., Collins, E.S., Gayes, P.T., Wright, E., 2003. Records of prehistoric hurricanes on the South Carolina coast based on micropaleontological and sedimentological evidence, with comparison to other Atlantic Coast records. GSA Bull. 115, 1027–1039. https://doi.org/10.1130/B25011.1.

Singleton, A.A., Schmidt, A.H., Bierman, P.R., Rood, D.H., Neilson, T.B., Greene, E.S., Bower, J.A., Perdrial, N., 2017. Effects of grain size, mineralogy, and acid-extractable grain coatings on the distribution of the fallout radionuclides 7Be, 10Be, 137Cs, and 210Pb in river sediment. Geochim. Cosmochim. Acta 197, 71–86.

Smith, A.B., Matthews, J.L., 2015. Quantifying uncertainty and variable sensitivity within the US billion-dollar weather and climate disaster cost estimates. Nat. Hazards 77 (3), 1829–1851. https://doi.org/10.1007/s11069-015-1678-x.

Smith, G.H., Best, J.L., Ashworth, P.J., Fielding, C.R., Goodbred, S.L., Prokocki, E.W., 2010. Fluvial form in modern continental sedimentary basins: distributive fluvial systems – comment. Geology 38 (12). https://doi.org/10.1130/G31507C.1 e230.

Stone, J.R., Cronin, T.M., Brewster-Wingard, G.L., Ishman, S.E., Wardlaw, B.R., Holmes, C.W., 2000. A paleoecologic reconstruction of the history of Featherbed Bank, Biscayne National Park, Biscayne Bay, Florida. *USGS OFR: 00-191*. https://doi.org/10.3133/ofr00191.

Sugg, A.L., Pardue, L.G., Carrodus, R.L., 1971. Memorable hurricanes of the United States since 1873. NOAA Technical Memorandum NWS SR, 56.

Sumner, H.C., 1947. North Atlantic hurricanes and tropical disturbances of 1947. Mon. Weather Rev. 75, 251–255. https://doi.org/10.1175/1520-0493(1947)075<0251:NAHATD>2.0.CO;2.

Trefry, J., Rember, R., Trocine, R., Woodall, D., 2004. Sedimentation Rates and Sediment Composition in Estero Bay. Florida: Executive Summary.

United States Census Bureau, 2019. Florida Quick Facts. Retrieved from. https://www.census.gov/quickfacts/FL.
Wang, R., Manausa, M., Cheng, J., 2005. Hurricane Charley Characteristics and Storm Tide Evaluation. Beaches and Shores Resource Center, Institute of Science and Public Affairs, Florida State University, Tallahassee, FL, USA.
Wohlpart, S.L., Savarese, M., Surge, D., 2007. The development of estuarine systems in Southwest Florida: a perspective from the late Holocene history of oyster reef development. Geol. Soc. Am. Abstr. Programs 39 (6), 182.
Woodruff, J.D., Donnelly, J.P., Mohrig, D., Geyer, W.R., 2008. Reconstructing relative flooding intensities responsible for hurricane-induced deposits from Laguna Playa Grande, Vieques, Puerto Rico. Geology 36 (5), 391–394. https://doi.org/10.1130/G24731A.1.